

REPORT DOCUMENTATION PAGE

Form Approved
OMB No. 0704-0188

Public reporting burden for this collection of information is estimated to average 1 hour per response, including the time for reviewing instructions, searching existing data sources, gathering and maintaining the data needed, and completing and reviewing this collection of information. Send comments regarding this burden estimate or any other aspect of this collection of information, including suggestions for reducing this burden to Department of Defense, Washington Headquarters Services, Directorate for Information Operations and Reports (0704-0188), 1215 Jefferson Davis Highway, Suite 1204, Arlington, VA 22202-4302. Respondents should be aware that notwithstanding any other provision of law, no person shall be subject to any penalty for failing to comply with a collection of information if it does not display a currently valid OMB control number. PLEASE DO NOT RETURN YOUR FORM TO THE ABOVE ADDRESS.

1. REPORT DATE (DD-MM-YYYY) 04-01-2006	REPRINT
--------------------------------------------------	----------------

4. TITLE AND SUBTITLE QUANTUM LATTICE REPRESENTATIONS FOR VECTOR SOLITONS IN EXTERNAL POTENTIALS	5a. CONTRACT NUMBER
	5b. GRANT NUMBER
	5c. PROGRAM ELEMENT NUMBER 61102F

6. AUTHOR(S) G. Vahala*, L. Vahala** and J. Yezep	5d. PROJECT NUMBER 2304
	5e. TASK NUMBER 0T
	5f. WORK UNIT NUMBER B1

7. PERFORMING ORGANIZATION NAME(S) AND ADDRESS(ES) Air Force Research Laboratory/VSBYA 29 Randolph Road Hanscom AFB MA 01731-3010	8. PERFORMING ORGANIZATION REPORT NUMBER AFRL-VS-HA-TR-2005-1202
---------------------------------------------------------------------------------------------------------------------------------------------------	--------------------------------------------------------------------------------

9. SPONSORING / MONITORING AGENCY NAME(S) AND ADDRESS(ES)	10. SPONSOR/MONITOR'S ACRONYM(S)
	11. SPONSOR/MONITOR'S REPORT NUMBER(S)

12. DISTRIBUTION / AVAILABILITY STATEMENT
Approved for Public Release; Distribution Unlimited.

*Dept Physics, William & Mary, Williamsburg, VA
**Dept Electrical & Computer Engr, Old Dominion Univ, Norfolk, VA

13. SUPPLEMENTARY NOTES
REPRINTED FROM: Physica A, doi:10.1016/j.physa.2005.09.029 (in press)

14. ABSTRACT

A quantum lattice algorithm is developed to examine the effect of an external potential well on exactly integrable vector Manakov solitons. It is found that the exact solutions to the coupled nonlinear Schrodinger equations act like quasi-solitons in weak potentials, leading to mode-locking, trapping and untrapping. Stronger potential wells will lead to the emission of radiation modes from the quasi-soliton initial conditions. If the external potential is applied to that particular mode polarization, then the radiation will be trapped within the potential well. The algorithm developed leads to a finite difference scheme that is unconditionally stable. The Manakov system in an external potential is very closely related to the Gross-Pitaevskii equation for the ground state wave functions of a coupled BEC state at $T = 0K$.

15. SUBJECT TERM:
Quantum lattice gas Solitons Manakov solitons
Nonlinear Schrodinger equation Gross-Pitaevskii equations Optical fibers

16. SECURITY CLASSIFICATION OF:		17. LIMITATION OF ABSTRACT	18. NUMBER OF PAGES	19a. NAME OF RESPONSIBLE PERSON Jeffrey Yezep
a. REPORT UNCLAS	b. THIS PAGE UNCLAS	SAR		19b. TELEPHONE NUMBER (include area code) 781-377-5957



ELSEVIER

Available online at www.sciencedirect.com

SCIENCE @ DIRECT®

Physica A ■■■■■■■■■■

PHYSICA A

www.elsevier.com/locate/physa

DTIC COPY

Quantum lattice representations for vector solitons in external potentials

George Vahala^{a,*}, Linda Vahala^b, Jeffrey Yezep^c^aDepartment of Physics, William & Mary, Williamsburg, VA 23187 USA^bDepartment of Electrical & Computer Engineering, Old Dominion University, Norfolk, VA 23529, USA^cAir Force Research Laboratory, Hanscom Field, MA 01731, USA

Abstract

A quantum lattice algorithm is developed to examine the effect of an external potential well on exactly integrable vector Manakov solitons. It is found that the exact solutions to the coupled nonlinear Schrodinger equations act like quasi-solitons in weak potentials, leading to mode-locking, trapping and untrapping. Stronger potential wells will lead to the emission of radiation modes from the quasi-soliton initial conditions. If the external potential is applied to that particular mode polarization, then the radiation will be trapped within the potential well. The algorithm developed leads to a finite difference scheme that is unconditionally stable. The Manakov system in an external potential is very closely related to the Gross-Pitaevskii equation for the ground state wave functions of a coupled BEC state at $T = 0$ K.

© 2005 Elsevier B.V. All rights reserved.

Keywords: Quantum lattice gas; Solitons; Manakov solitons; Nonlinear Schrodinger equation; Gross-Pitaevskii equation; Optical fibers

1. Introduction

In optical propagation down a birefringent fiber, under appropriate conditions [1] the two orthogonal polarization amplitudes satisfy the coupled nonlinear Schrodinger equations (NLS)

$$\begin{aligned} i\partial_t Q_1 + \partial_{xx} Q_1 + 2(|Q_1|^2 + B|Q_2|^2)Q_1 &= 0, \\ i\partial_t Q_2 + \partial_{xx} Q_2 + 2(|Q_2|^2 + B|Q_1|^2)Q_2 &= 0, \end{aligned} \quad (1)$$

where B is the cross-phase modulation coefficient (XPM): $B = (2 + 2\sin^2\theta)/(2 + \cos^2\theta)$ and θ is the birefringence angle of the fiber. For $B = 1$, Eq. (1) is exactly integrable by the inverse scattering as well as the Hirota method to yield the so-called Manakov vector solitons. Vector solitons have a richer behavior than their scalar counterparts that remain invariant in amplitude and speed under soliton-soliton collision. The only signature of a scalar soliton collision is an induced phase shift. However, in vector 2-soliton interactions, depending on the initial amplitudes, there exists the possibility of inelastic collisions [2].

*Corresponding author. Tel.: +1 757 221 3528; fax: +1 757 221 3540.

E-mail address: vahala@niv.physics.wm.edu (G. Vahala).

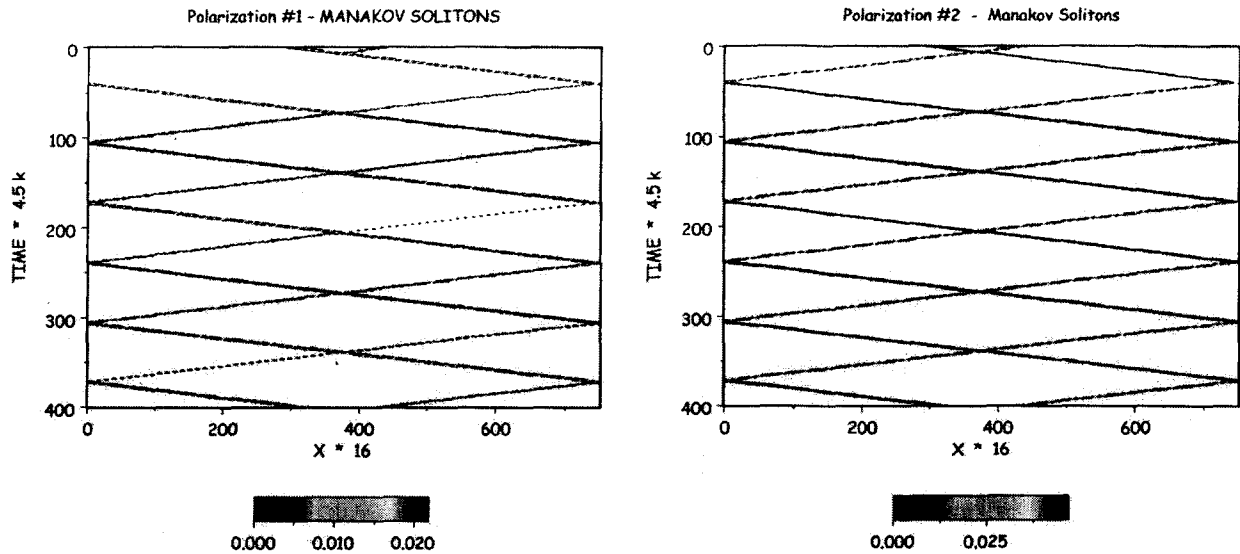


Fig. 1. Long time evolution of the Manakov soliton amplitudes $|Q_1|$ and $|Q_2|$ under periodic boundary conditions. Time increases vertically down. The total intensity in each mode is numerically preserved by our algorithm to better than 1 part in 10^7 . All soliton speeds are equal and are invariant under collisions. Soliton amplitudes are invariant in-between collisions and can be changed by a collision, subject to conservation of the total intensity in each mode.

If one employs periodic boundary conditions (which permits many $Q_1 - Q_2$ soliton collisions), there is on the next collision the re-appearance of the soliton destroyed in the first collision as can be seen in the long time evolution of the Manakov solitons Fig. 1.

The 4 soliton speeds are time-invariant, with only their amplitudes being affected by the collisions subject to constant total intensity in each mode. For the parameters chosen the soliton collisions always occur at the end point(s) and at the mid-point (on ignoring the very small collision-induced phase shifts). Furthermore, the corresponding right-traveling solitons from each polarization are mode-locked and similarly for the corresponding left-traveling solitons: i.e., the center of mass of each right-traveling soliton in the two polarizations are coincident (as are the center of masses for the left-traveling solitons).

Here we shall consider the effect of slowly (spatially) varying external potentials on this vector Manakov system

$$\begin{aligned} i\partial_t Q_1 + \partial_{xx} Q_1 + 2(|Q_1|^2 + |Q_2|^2)Q_1 + V_1^{\text{ext}}(x)Q_1 &= 0, \\ i\partial_t Q_2 + \partial_{xx} Q_2 + 2(|Q_2|^2 + |Q_1|^2)Q_2 + V_2^{\text{ext}}(x)Q_2 &= 0. \end{aligned} \quad (2)$$

For nonzero external potentials, the Manakov soliton solutions of Eq. (1) can at best be quasi-solitons since Eq. (2) is now nonintegrable. It is precisely this that we shall investigate here, keeping in mind that Eq. (2) bears a striking resemblance to the Gross-Pitaevskii [1] equation that describes the ground state wave function for the Bose-Einstein condensate (BEC) state at $T = 0$ K in an external confining potential.

2. Vector Manakov equations in external potentials

A quantum lattice representation for the vector Manakov system Eq. (1) has been presented in detail in Ref. [3] so we shall only briefly describe the algorithm here. After discretizing the spatial domain one introduces 2 qubits/node for each polarization mode. Since the diffusive part of Eq. (1) does not couple the polarizations Q_1 and Q_2 , this can be recovered from the quantum lattice algorithm by simply collisionally entangling just the 2 qubits of the same polarization mode at each spatial node. The required unitary collide-stream

sequence is [3]

$$\begin{pmatrix} Q_1(t + \Delta t) \\ Q_2(t + \Delta t) \end{pmatrix} = \begin{pmatrix} [S_2^T C S_2 C S_2^T C S_2 C S_1^T C S_1 C S_1^T C S_1 C] Q_1(t) \\ [S_4^T C S_4 C S_4^T C S_4 C S_3^T C S_3 C S_3^T C S_3 C] Q_2(t) \end{pmatrix}, \quad (3)$$

where the global unitary collision operator C is a tensor product of the local $\sqrt{\text{SWAP}}$ gate that entangles the 2 qubits of each polarization separately, while the streaming operator on qubit “ i ” spreads this entanglement throughout the lattice. S_i streams qubit “ i ” to the right while S_i^T streams qubit “ i ” to the left. The symmetrizing of the algorithm on qubits “1”–“2” and qubits “3”–“4” will result in a higher-order accurate finite difference scheme. In the continuum limit under diffusive ordering, $\Delta x^2 = O(\varepsilon^2) = \Delta t$, Eq. (3) yields the uncoupled free-Schrodinger equations for the polarization modes. (Δx is the lattice cellsize) [4]. The nonlinear coupling of the polarizations is readily obtained by introducing appropriate phase modulations into the polarization wave functions Q_1 and Q_2 . This can be understood from path integral formulations of quantum mechanics or from multiscattering theory of classical electromagnetic wave propagation [5] in which phase modulations are introduced and then converted into amplitude modulations by the diffusive part of the parabolic Schrodinger equation. Thus, with the phase modulation

$$\begin{pmatrix} Q_1 \\ Q_2 \end{pmatrix} \rightarrow \begin{pmatrix} e^{iV_1(|Q_1|, |Q_2|)\Delta t} & 0 \\ 0 & e^{iV_2(|Q_1|, |Q_2|)\Delta t} \end{pmatrix} \begin{pmatrix} Q_1 \\ Q_2 \end{pmatrix} \quad (4)$$

applied following the unitary collide-stream operator sequence, Eq. (3), one obtains in the continuum limit

$$\begin{aligned} i\partial_t Q_1 + \partial_{xx} Q_1 + V_1(|Q_1|, |Q_2|)Q_1 + O(\varepsilon^2) &= 0, \\ i\partial_t Q_2 + \partial_{xx} Q_2 + V_2(|Q_1|, |Q_2|)Q_2 + O(\varepsilon^2) &= 0, \end{aligned} \quad (5)$$

where the potentials V_i ($i = 1, 2$) are arbitrary functions of the polarization wave functions and/or space. A particular choice of these potentials thus yields the required vector Manakov equations inn external potentials, Eq. (2).

3. Manakov quasi-solitons in an external potential well

Taking as initial conditions the Manakov solitons of Fig. 1, the role of an external potential well of depth U_0 on the subsequent time evolution is considered, with

$$V_{\text{ext}}(x) = U_0 \tanh^2\left(\frac{x - L_x/2}{L_x/5}\right), \quad 0 \leq x < L_x \quad (6)$$

V_{ext} is symmetric about $L_x/2$ where it is zero, and then gently asymptotes to U_0 as $x \rightarrow 0$ or L_x .

We first consider the effect of a very weak potential well on the polarization mode Q_1 only: i.e., Eq. (2) with $V_1^{\text{ext}}(x) = V_{\text{ext}}(x)$, and $V_2^{\text{ext}}(x) = 0$. Here, the potential well U_0 is an order of magnitude smaller than the amplitude of the smallest initial soliton in Fig. 1. The external potential is sufficiently weak that the initial conditions yield quasi-solitons that retain their identity under collisions and there is mode-locking of the quasi-solitons. However, the external potential creates enough perturbation that both quasi-solitons of mode Q_1 now still exist after the first collision. Since the quasi-solitons are mode-locked, one need only present the long time evolution for one of the polarization modes. In Fig. 2, we plot the evolution of the quasi-solitons of mode Q_2 . The initially right traveling quasi-soliton undergoes an amplitude modulation after the 1st collision and then becomes trapped in the weak potential well ($t = 50 \times 4.5$ k). It then moves to the left, parallel with the other soliton (which is always untrapped) and reflects off the right potential wall ($t = 105 \times 4.5$ k). However, after the next collision (around $t = 150 \times 4.5$ k) this quasi-soliton becomes untrapped and stays untrapped for all times.

The same very weak external potential is now applied to mode 2, with no external potential on mode 1: $V_1^{\text{ext}}(x) = 0$, and $V_2^{\text{ext}}(x) = V_{\text{ext}}(x)$. Because the initial state for mode 2 is very different from that for mode 1, the effect of the external potential on mode 2 will be different from that on mode 1. The run time is now extended to 3.6 M iterations and is plotted in Fig. 3 in two parts: $0 < t < 1.8$ M, and 1.8 M $< t < 3.6$ M. Again,

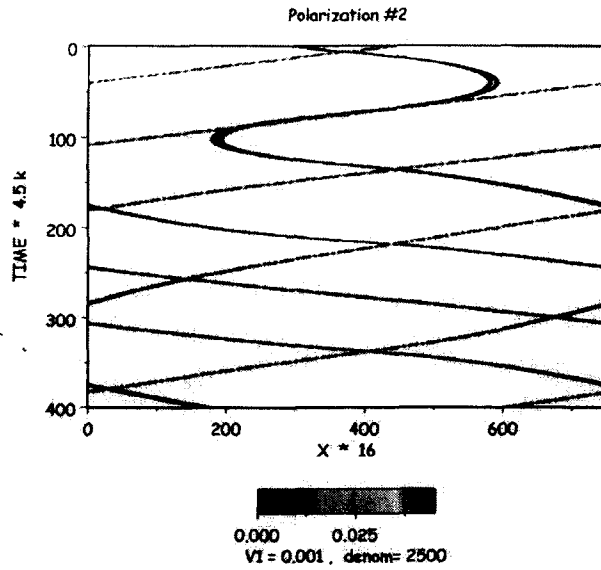


Fig. 2. The effect of a very weak external potential well on mode 1. The quasi-solitons are mode-locked so only the time evolution of mode 2 is presented. After the 1st collision the right traveling quasi-soliton is trapped by the potential well, but it escapes from the well after basically one period. The initial left-traveling quasi-soliton is always untrapped.

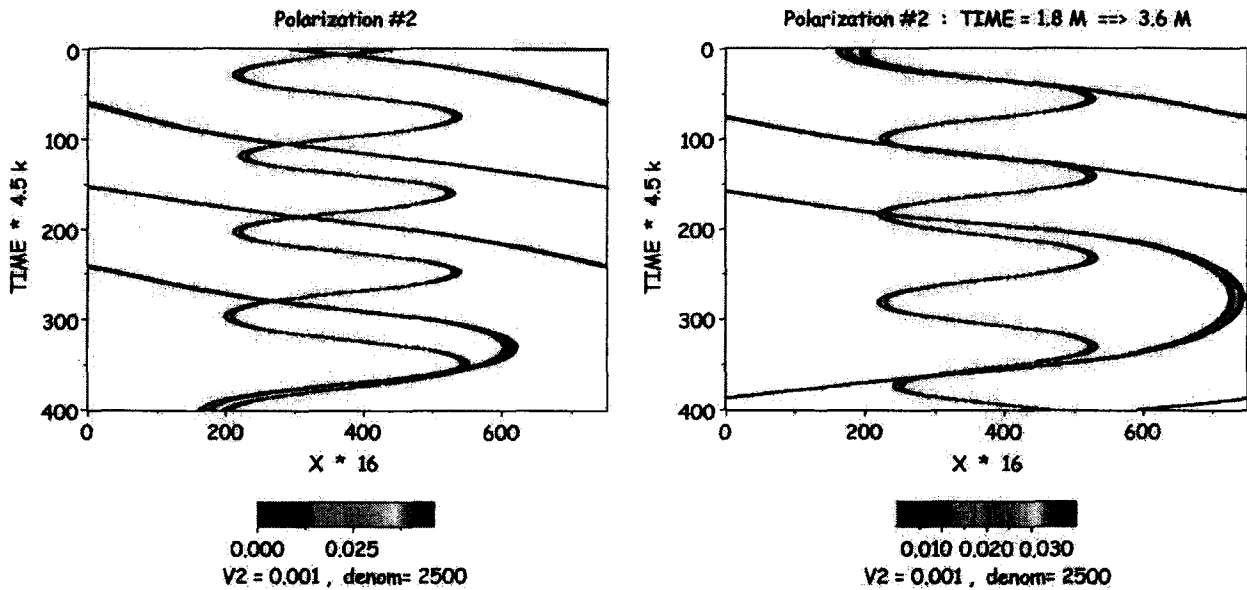


Fig. 3. The effect of the same very weak external potential well as in Fig. 1, but now only on mode 2. The quasi-solitons are mode-locked so only the time evolution of mode 2 is presented, but this time for twice the number of iterations plotted in Fig. 2. It is now the initially left-moving quasi-soliton that is trapped and remains trapped by the external potential for all time, $0 < t < 3.6M$. On the other hand, the initially right moving soliton becomes trapped (around $t = 340 \times 4.5k$) for one period, and then becomes untrapped and then eventually retrapped ($t = 1.8M + 300 \times 4.5k$).

the quasi-solitons are mode-locked and so results are presented only for mode 2. The left-moving quasi-soliton at $t = 0$ remains trapped by this very weak potential well for all time, $0 < t < 3.6M$. On the other hand, the $t = 0$ right-moving quasi-soliton undergoes several untrapped-trapped sequences.

The strength of the potential well is now increased by a factor of 2.5. Again the resulting quasi-soliton motion is mode-locked and we present the results on mode polarization 1. For early times, $0 < t < 265 \times 4.5 \text{ k}$, the potential well is sufficiently deep that both initial quasi-solitons are trapped. However, for later times there is an intricate intertwined sequence of trapped-untrapped that occurs among the quasi-solitons, as seen in Fig. 4. If the potential well is now applied to the polarization mode Q_2 rather than to Q_1 , the two

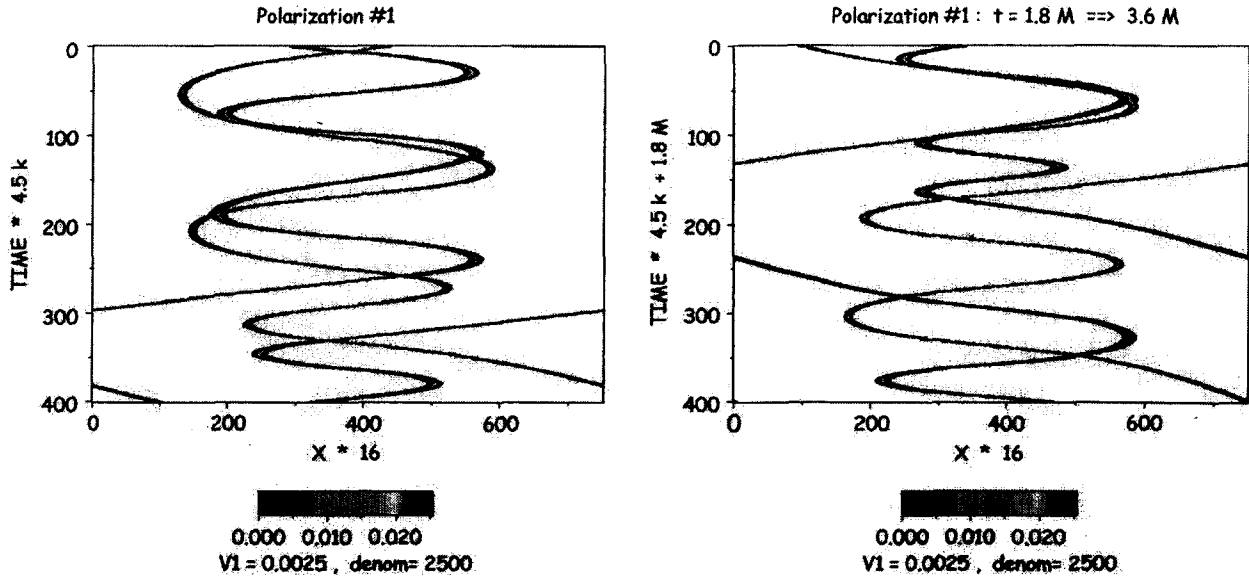


Fig. 4. The effect of increasing the potential well by a factor of 2.5. The quasi-solitons are still mode-locked for polarizations 1 and 2. With the same initial conditions for all runs reported in this paper, we now find that the quasi-solitons are initially trapped and after more collisions an interweaving alternating web between the two quasi-solitons of trapped-untrapped.

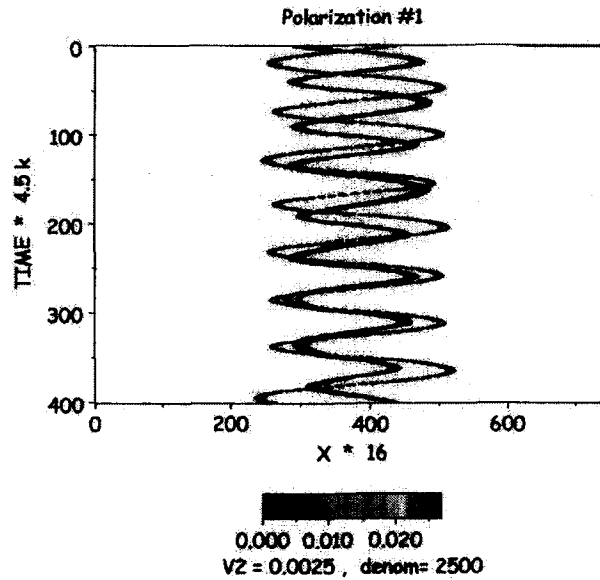


Fig. 5. The same external potential as in Fig. 4, but now applied to the polarization mode Q_2 . Again there is mode-locking between the two polarization modes Q_1 and Q_2 . The evolution of the quasi-solitons for mode Q_1 are plotted up to time $t = 1.8 \text{ M}$, and both quasi-solitons are trapped within the potential well. The difference between Figs. 4 and 5 arise from the application of the external potential to different polarization mode initial quasi-soliton amplitudes.

quasi-solitons are trapped for all times, shown in Fig. 5. The external potential is now increased by a factor of 5 over that in Fig. 3. It is applied to polarization mode Q_2 only. In Fig. 6 we plot the evolution of the initial quasi-solitons for both mode Q_1 (with no external potential) and mode Q_2 . For times $t < 170 \times 4.5$ k, there is mode-locking between the Q_1 and Q_2 polarizations. Shortly after this one starts to see radiation modes between spewed out in the Q_1 polarization and eventually these modes are unconfined (Fig. 7 for $t = 300 \times 4.5$ k). However, for polarization Q_2 radiation modes are emitted later in time but they are confined by the potential well applied to Q_2 (Fig. 7b for $t = 300 \times 4.5$ k). For $t > 350 \times 4.5$ k, quite strong radiation modes are emitted in the Q_2 polarization, but they are confined by the potential well. As the external potential well is increased, so will the potential gradients until eventually the $t = 0$ quasi-solitons are completely destroyed and only radiation modes exist. If the external potential is applied to polarization Q_i then the

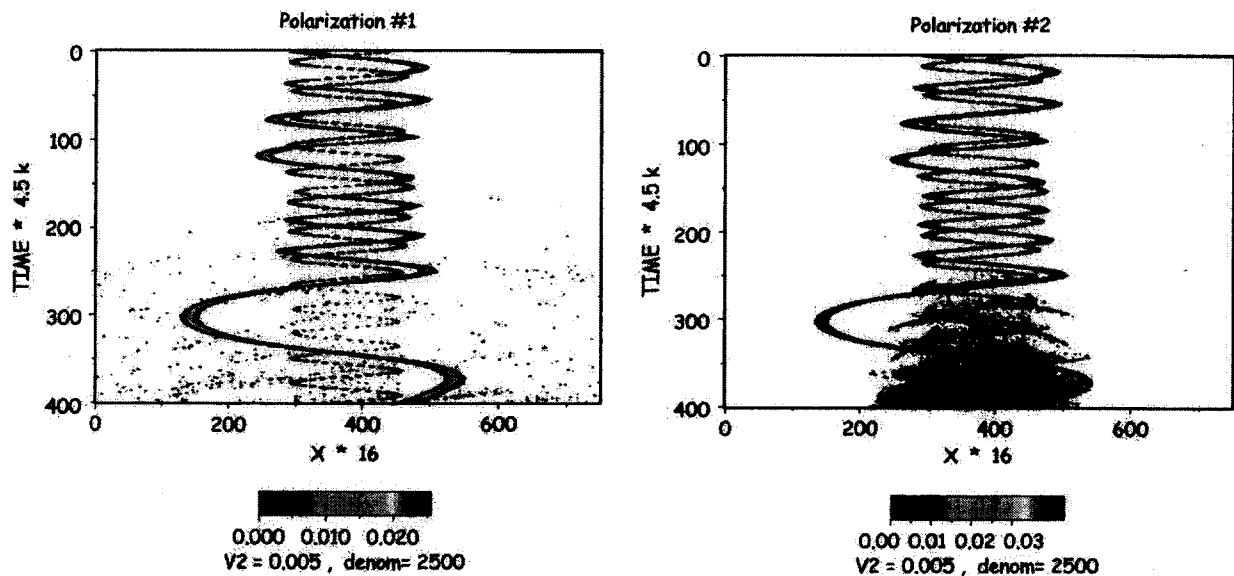


Fig. 6. The mode locking of Q_1 with Q_2 is broken for $t > 170 \times 4.5$ k, with radiation emission in both Q_1 and Q_2 . For Q_1 the radiation is untrapped, while trapped for Q_2 .

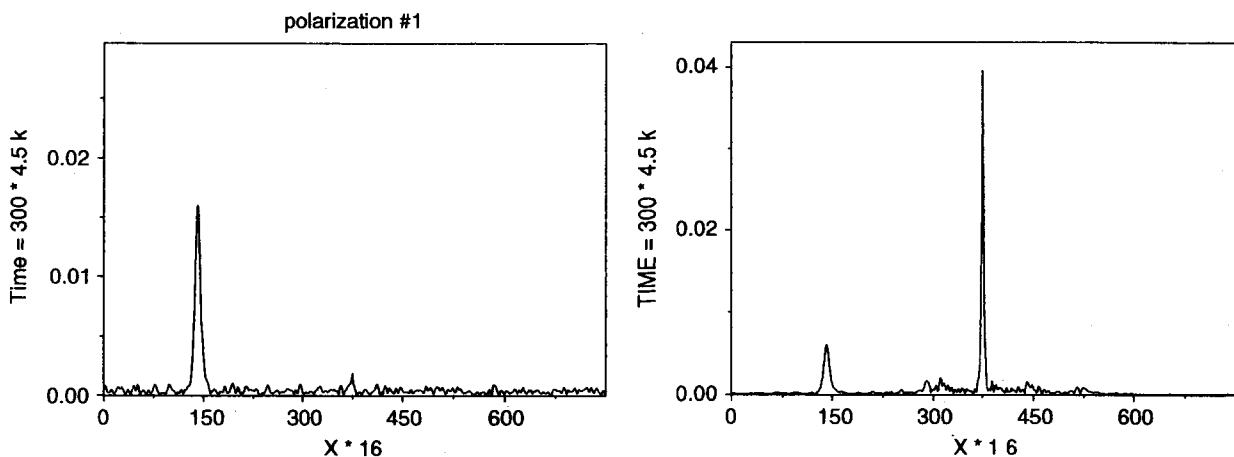


Fig. 7. A snapshot at time $t = 300 \times 4.5$ k of $|Q_1|$ and $|Q_2|$ with the external potential only applied to polarization Q_2 . The quasi-soliton structures still exist and are mode-locked for the polarizations (located around $x = 150 \times 16$ and $x = 375 \times 16$). However, radiation modes are also emitted in both the Q_1 and Q_2 solutions. In the case of Q_1 the radiation occurs throughout the entire lattice while for Q_2 the radiation is spatially confined by the potential well (here to the region $225 \times 16 < x < 550 \times 16$).

radiation modes generated with the collapse of the initial quasi-solitons will be trapped by the external potential.

4. Conclusion

A quantum lattice representation for vector solitons in an external potential has been developed. The algorithm employs a sequence of unitary collision operators ($\sqrt{\text{SWAP}}$ gate) that locally entangle the qubits at each node and unitary streaming operators that rapidly spreads this entanglement through the lattice. It will be difficult to implement our quantum algorithm experimentally. First, the quantum phase coherence must be maintained throughout the complete sequence of collide-stream, Eq. (3). This must then be followed by quantum measurement from which we need to extract the absolute values of the amplitudes and not simply the probabilities which are naturally extracted from the projective von Neumann quantum measurement over a large ensemble. This is how the nonlinear interaction potentials are determined, Eq. (4). Our quantum lattice algorithm gives rise to a finite difference scheme that is explicit and unconditionally stable. Moreover, the quantum algorithm is very efficiently parallelized on a classical computer.

References

- [1] Y.S. Kivshar, G.P. Agrawal, *Optical Solitons*, Academic Press, New York, 2003.
- [2] R. Radhakrishnan, M. Lakshmanan, J. Hietarinta, *Phys. Rev. E* 56 (1997) 2213.
- [3] G. Vahala, L. Vahala, J. Yepez, Inelastic vector soliton collisions: a lattice-based quantum representation, *Philos. Trans. Roc. Soc.* 362 (1821) (2004) 1677–1690.
- [4] J. Yepez, B. Boghosian, An efficient and accurate quantum lattice-gas model for the many-body schrodinger wave equation, *Comput. Phys. Commun.* 146 (3) (2002) 280–294.
- [5] B. Uscinski, *The Elements of Wave Propagation in Random Media*, Academic Press, New York, 1977.